

Supplemental information

**Colocalization of different neurotransmitter
transporters on synaptic vesicles is sparse
except for VGLUT1 and ZnT3**

Neha Upmanyu, Jialin Jin, Henrik von der Emde, Marcelo Ganzella, Leon Bösche, Viveka Nand Malviya, Evi Zhuleku, Antonio Zaccaria Politi, Momchil Ninov, Ivan Silbern, Marcel Leutenegger, Henning Urlaub, Dietmar Riedel, Julia Preobraschenski, Ira Milosevic, Stefan W. Hell, Reinhard Jahn, and Sivakumar Sambandan

SUPPLEMENTAL INFORMATION

Supplemental Figures

Figure S1, related to Introduction and Figure 3

Figure S2, related to Figure 1

Figure S3, related to Figure 1, 2

Figure S4, related to Figure 1, 2

Figure S5, related to Figure 2 and STAR Methods

Figure S6, related to Figure 2, 3, 5

Figure S7, related to Figure 6

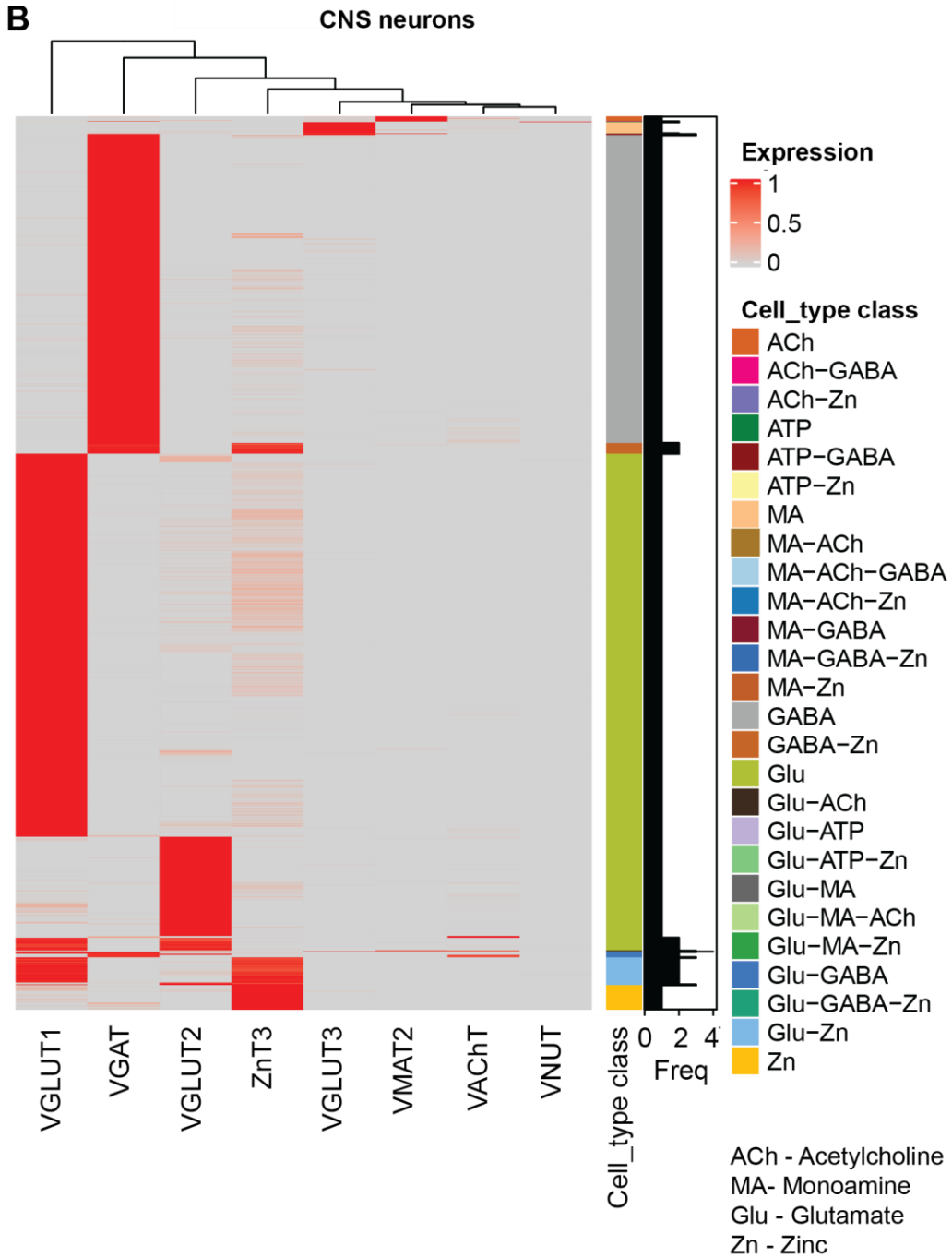
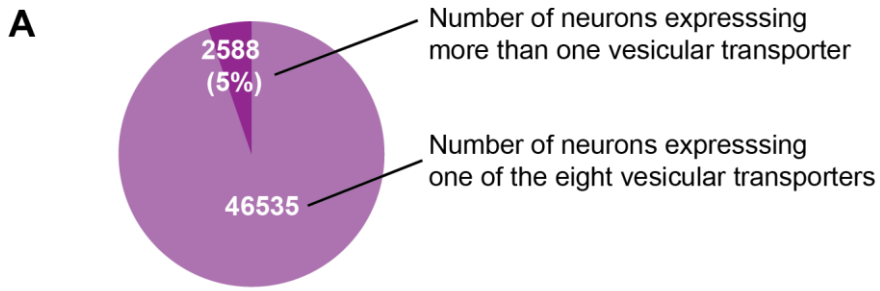


Figure S1. Coexpression of vesicular transporters in the whole brain revealed by single cell transcriptome analysis

(A) Pie diagram showing the composition of neurons in the whole brain expressing more than one vesicular transporter (total neurons analyzed = 70968; neurons expressing at least one transporter = 49123) (B) Heat map showing the normalized co-expression of different vesicular transporter genes. Horizontal lines represent single neurons expressing either one or multiple vesicular transporters shown on the X-axis. The heat map color ranges from grey to red (0 to 1); grey indicates no expression and red intensity shows the expression level of genes. The color bar on the right shows the assigned cell types based on the expression of one or more types of transporters. Bar plot (black) represents the number of transporter genes expressed in the cell type on the left. Note that cell types expressing three or even four different transporters are also identified. The transcriptome data is reanalyzed from Zeisel et al., 2018.

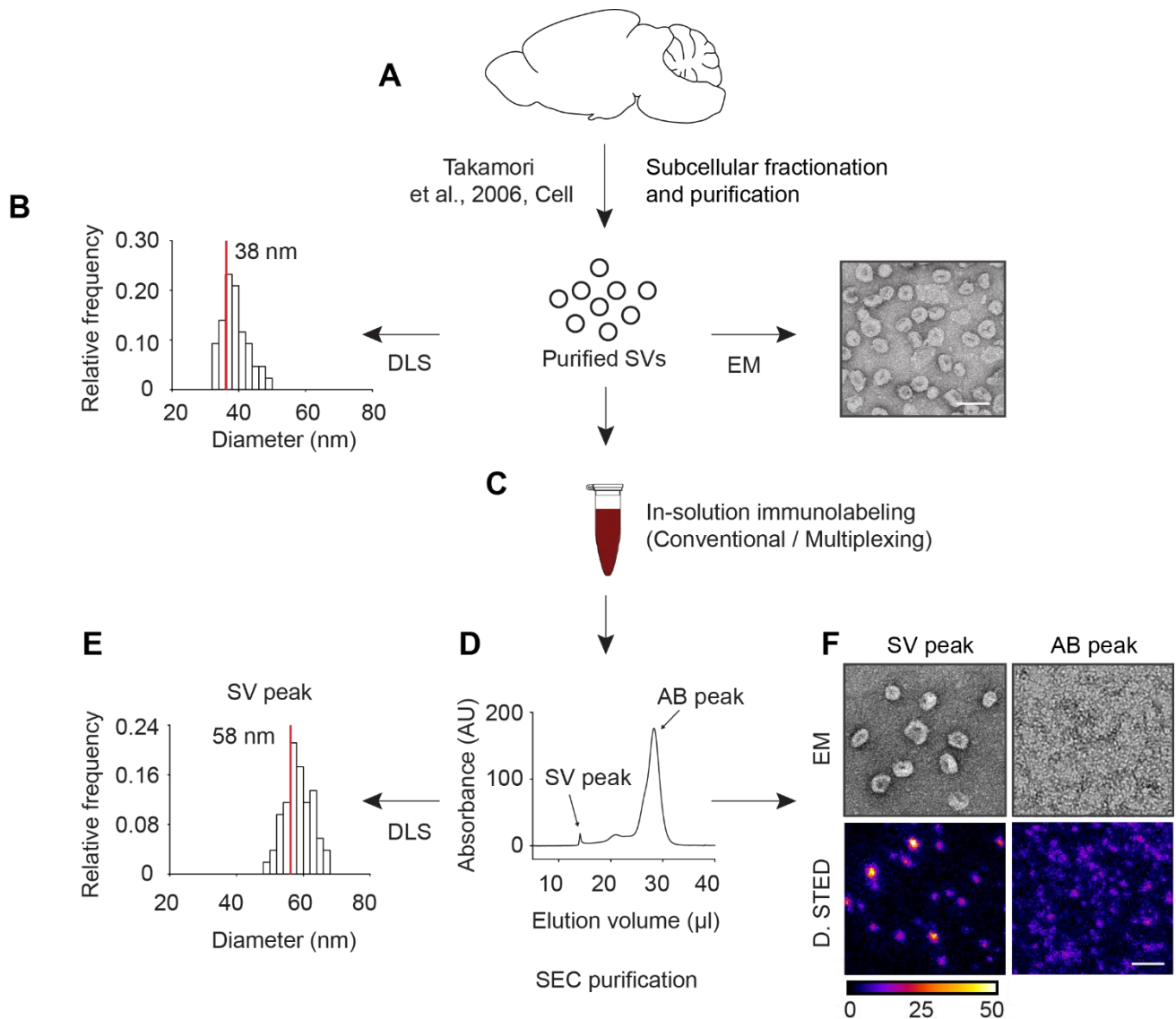


Figure S2. Overview of the workflow of synaptic vesicle isolation, labeling and further purification for DyMIN STED single-vesicle imaging

(A) Purified SVs were prepared by a multi-step subcellular fractionation, as described in Takamori et al., 2006. (B) The purity and homogeneity of isolated SVs was tested using electron microscopy (EM, representative image on the right) and diffraction light scattering (DLS, summary histogram of particle diameter on the left). The mean size of individual SVs, as measured by DLS particle diameter was ~ 38 nm ($n = 22$ experiments). DLS particle count was used as a measure for the concentration of individual vesicles in the further steps. Scale bar, 50 nm. (C) After a blocking step, isolated SVs were incubated with saturating antibody concentration ‘in-solution’ under constant rotation for 1 h. (D) The immunolabeled SVs were then subjected to size exclusion chromatography (SEC) to remove unbound free antibodies and other contaminants such as excess serum proteins in the blocking buffer. Representative chromatogram demonstrates clear separation between the labeled SVs (SV peak) that was eluted in void volume and the contaminants (AB peak). (E) The quality of SEC purification was verified by subjecting the SV and AB peaks for DLS measurements in all experiments. Note that the mean size of SVs (red line in the DLS histogram) is increased (~ 20 nm) following immunolabeling indicating the change in size of SVs due to the bound antibodies. DLS measurement was not possible in the AB peak because of the heterogeneous particle size. (F)

In some experiments, EM and DyMIN STED were used to examine SV and AB peaks following direct immunolabeling of SVs. As expected, only the SV peak contained detectable SVs in the EM, whereas fluorescence was detected in both the samples. The labeled SVs were then immobilized on glass coverslips to prepare for DyMIN STED. Scale bar, 100nm

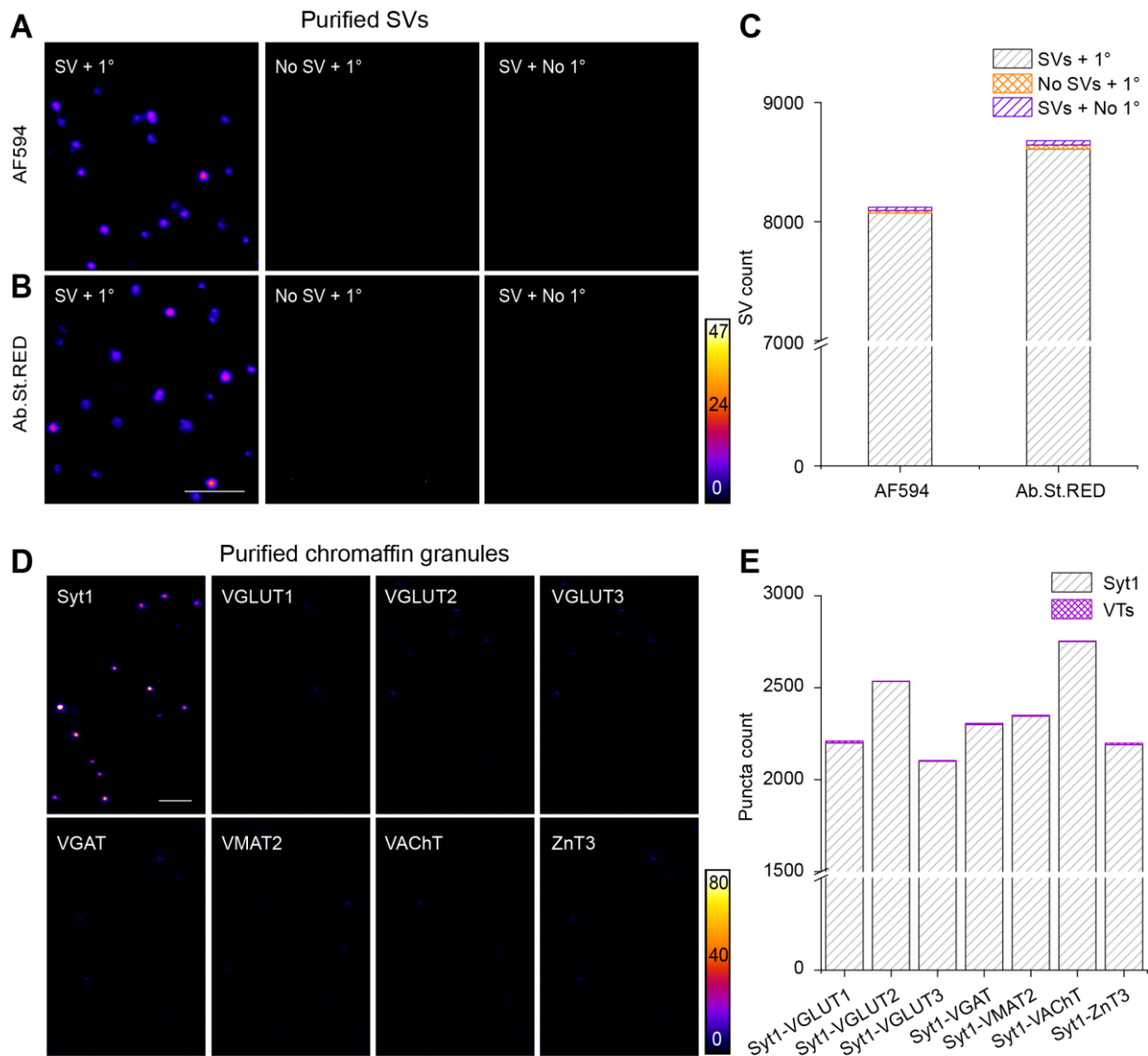


Figure S3. Marginal background and unspecific fluorescence in DyMIN STED single vesicle imaging

(A) Left, representative DyMIN STED images (fire) of purified SVs labeled against Syb2 using mouse anti-Syb2 primary antibody and anti-mouse secondary antibody conjugated with Alexa Fluor 594 (AF594). Middle, image showing undetectable fluorescence when SVs were omitted but all other staining steps kept unchanged. Right, image showing undetectable fluorescence when the primary antibody was omitted but all other staining steps were left unimpaired. (B) Similar representations as shown in A except that the secondary antibody was conjugated to Abberior Star Red (Ab.St.RED). Scale bar, 500 nm. (C) Stacked column graph showing negligible fluorescence ($\sim 0.1\%$) when either the SV (orange) or the primary antibody (magenta) was omitted during the staining ($n = 5$ independent experiments for both Ab.St.RED and AF594). (D) Representative images (fire) of Synaptotagmin 1 (Syt1) and specified VTs in purified chromaffin granules (CGs). Syt1, which is endogenously present on CGs was used as a marker for CGs. Scale bar = 500 nm. (E) Stacked column graph shows quantification of the number of puncta for the indicated combinations of antibodies.

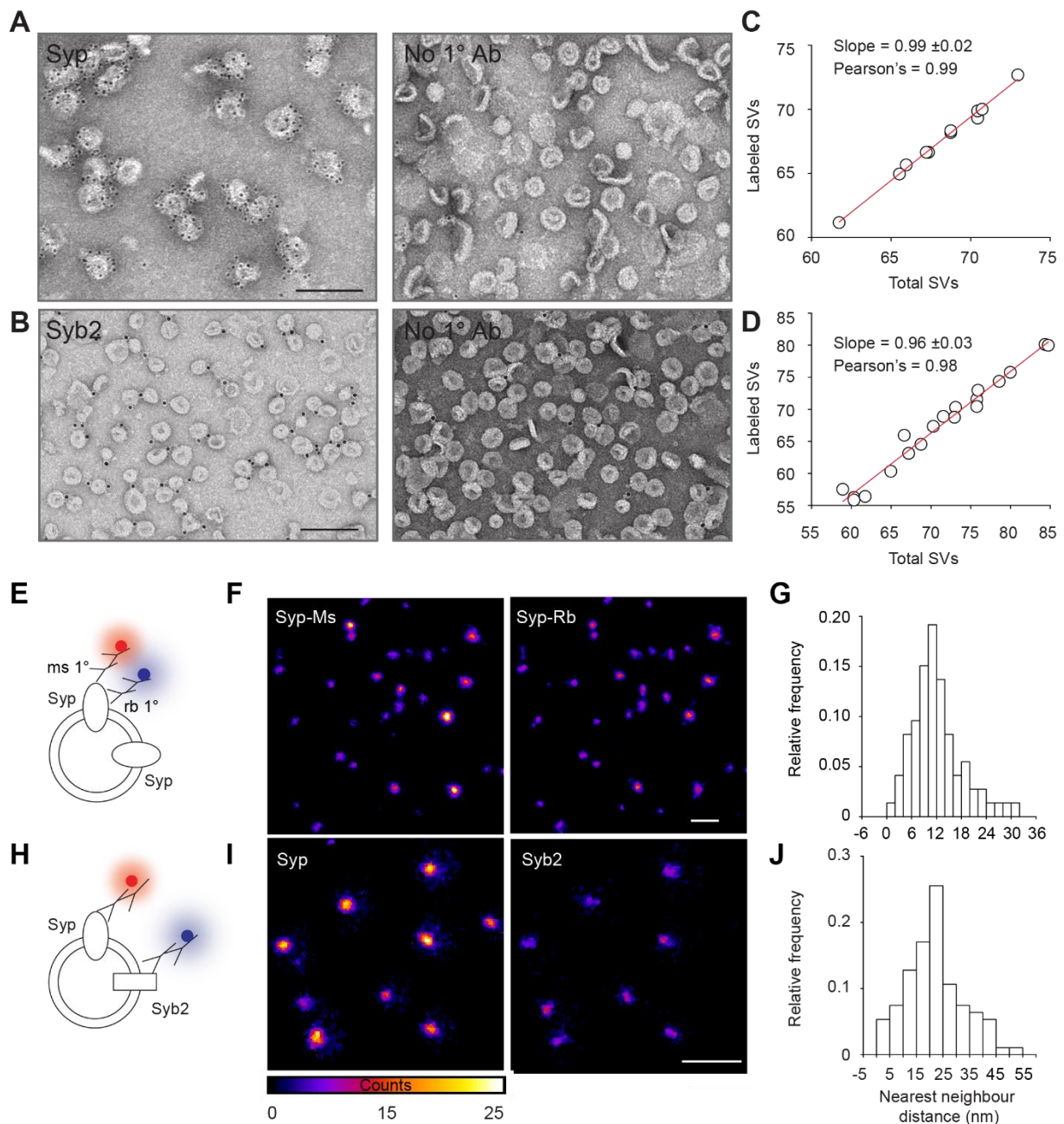


Figure S4. Immunogold electron microscopy (IEM) and two-color DyMIN STED reveals Syp and Syb2 as markers for the total number of SVs

(A) Representative immunogold electron microscopy (IEM) image of purified SVs labeled against Syp. (B) Representative IEM image of purified SVs labeled against Syb2. The images on the right represent the negative controls that lack the respective primary antibodies. Anti-Syp antibody typically labeled all small vesicular profiles with ~ 10 gold particles per vesicle. Anti-Syb2 antibody labeled $\sim 96\%$ of vesicles but mostly with only 1 gold particle per vesicle. Scale bars in A and B, 100 nm. (C) and (D) Scatter plots quantifying the labeled SVs for Syp and Syb2 in IEM. Total SVs (X-axis) are plotted against gold-labeled SVs (Y-axis) in individual images. Data points were fitted to a linear model ($n = 2$ experiments). Labeling of almost all SVs by Syp and Syb2 antibodies in IEM, which exhibits limited labeling efficiency, increases the likelihood that the two antibodies stain all SVs in DyMIN STED imaging, which exhibits supra-optimal conditions because of in-solution immunolabeling. (E) Illustration depicting two-color labeling of the same protein, Syp, in purified SVs using mouse and rabbit anti-Syp

primary antibodies. **(F)** Representative DyMIN STED images (fire) of the two fluorescence channels. Scale bar, 500 nm **(G)** Histogram showing the distribution of nearest neighbor distances (NND) of Syp-Ms puncta in Syb2-Rb channel. **(H)** Illustration depicting double immunolabeling of SVs against Syp and Syb2. **(I)** Representative DyMIN STED images showing single vesicles expressing Syp (left) and Syb2 (right). Scale bars in F and I, 500 nm **(J)** Histogram showing the distribution of nearest neighbor distances of Syp puncta in Syb2 channel. Note the distances between centers of all puncta in G and H is <55 nm, which allowed setting a threshold for the distance between the coordinates of two fluorescence puncta for the determination of colocalization of proteins on the same SVs ($n = 4$ experiments, $>14,000$ SVs in each channel).

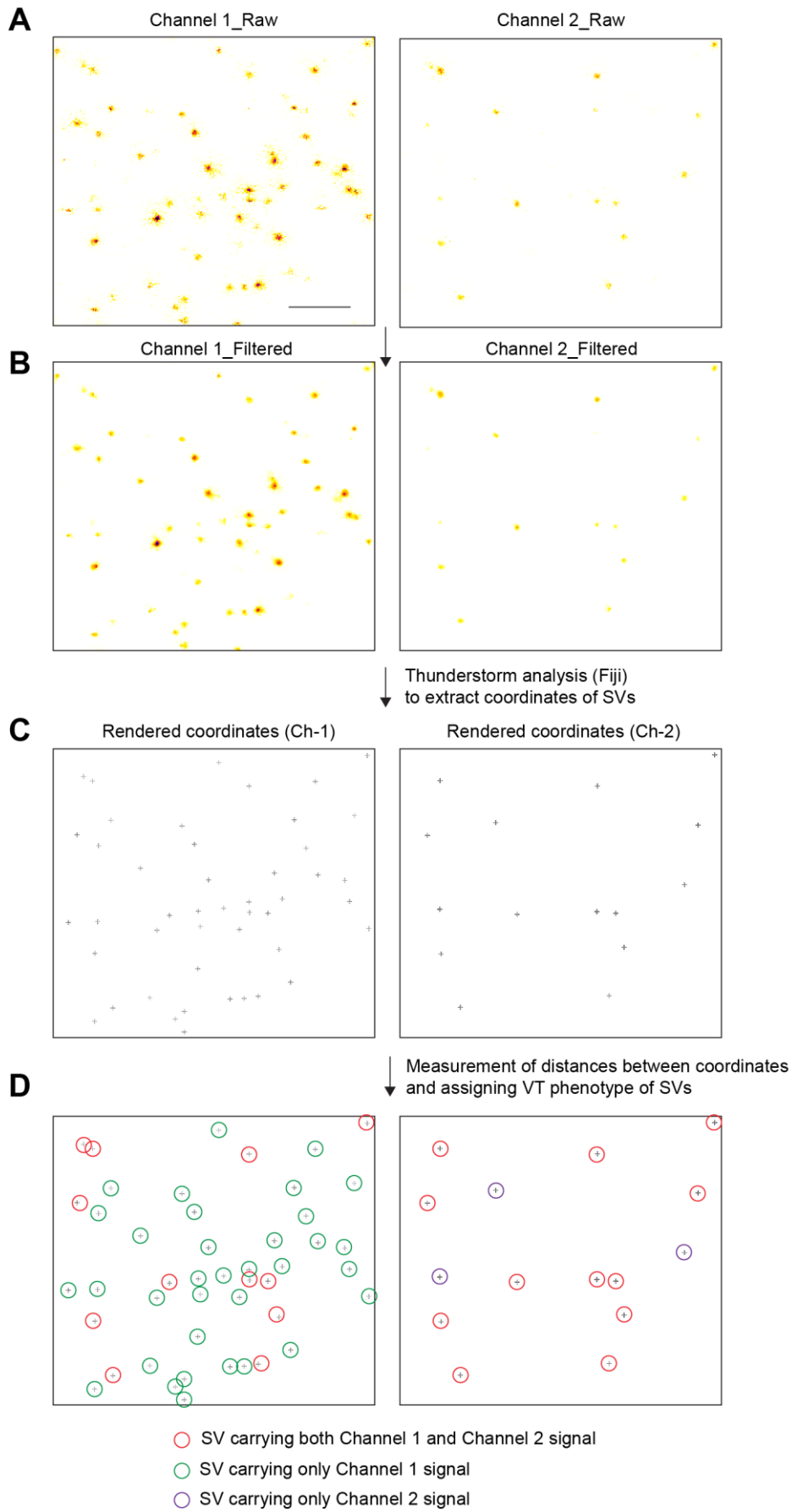


Figure S5. Overview of single vesicle colocalization analysis workflow

(A) Representative raw images (inverse color map) of an example two-channel DyMIN STED acquisition of single vesicles labeled against two SV proteins (Channel 1 and Channel 2). Scale bar, 500 nm. (B) Same paired images as above are shown following median filtering with a radius of 1 pixel (15 nm). (C) Rendering of the paired images above showing extracted coordinates of detected puncta using Thunderstorm analysis, an open source Plugin in Fiji. (D) The distance between the coordinates of any two puncta and in paired images was calculated. Two proteins were considered as colocalized on the same vesicle if the distance between the coordinates is less than 50 nm (see Figure S4 for details), yielding VT phenotype of detected SVs and their corresponding percentage composition.

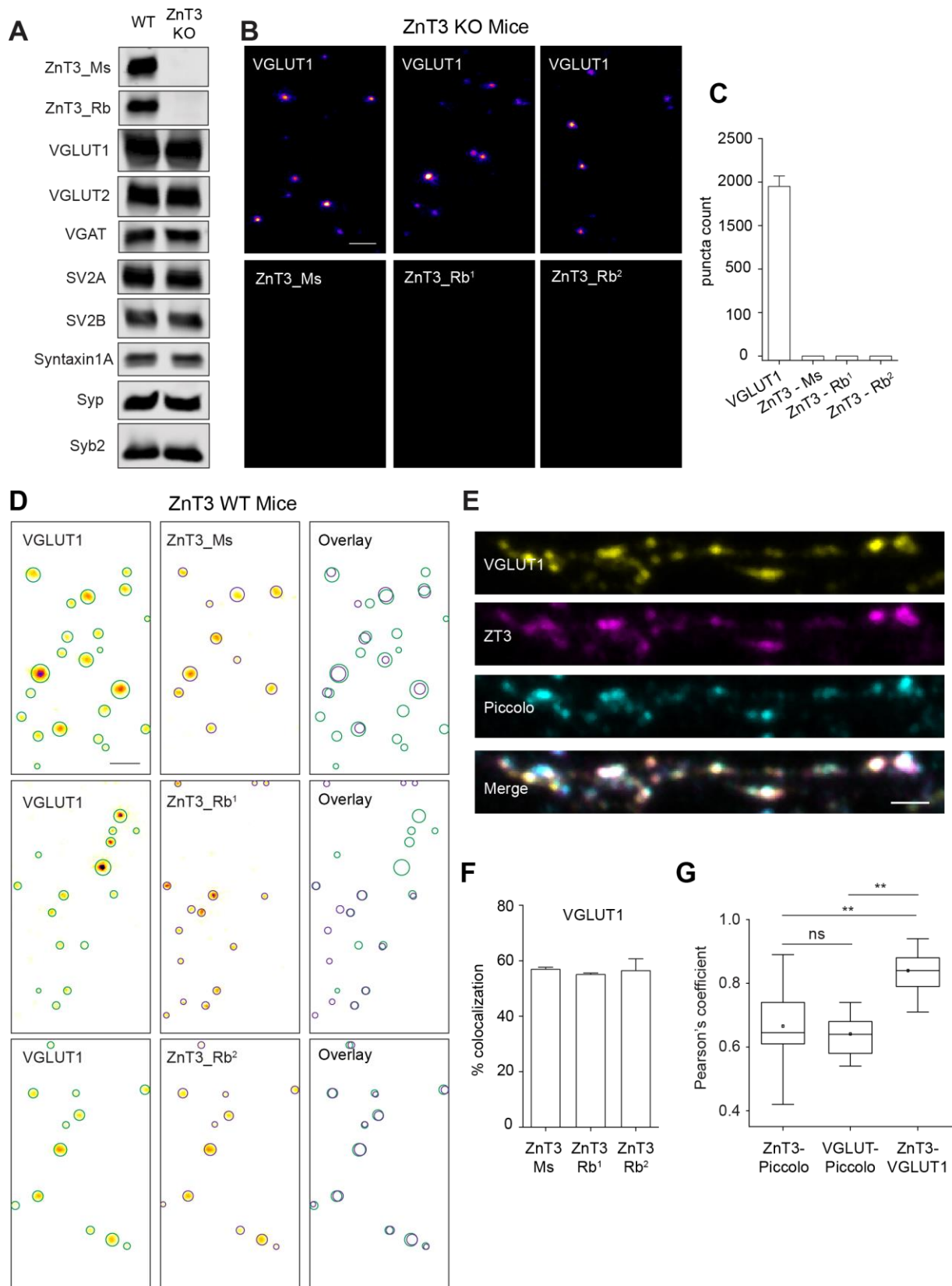


Figure S6. Validation of robust VGLUT1 and ZnT3 colocalization in mouse preparations and hippocampal culture neurons

(A) Western blot detection of ZnT3 and other selected SV proteins in wild type (WT) and ZnT3 knock out (KO) SV preparations (LP2). Both mouse and rabbit antibodies against ZnT3 (Ms-SySy-197011; Rb¹- SySy- 197003) were not able to detect any ZnT3 in the KO derived sample,

thus validating the specificity of ZnT3 antibodies used in the current study. However, there was no apparent difference in the expression of other proteins tested in the KO mice, including VGLUT1. **(B)** Representative images of single VGLUT1 and ZnT3 SVs purified from ZnT3 KO mice for the specified antibodies (Ms- SySy-197011; Rb¹- SySy- 197003; Rb²- Alomone Labs-AZT-013). **(C)** Bar graph showing quantification of VGLUT1 and ZnT3 SVs in the KO **(D)** Representative two-color DyMIN STED images (inverse color map) of VGLUT1 and ZnT3 (specified antibodies) channels in the wildtype. Circles portray SV area derived by a 2D Gaussian fit on VGLUT1 (green) and ZnT3 (magenta) puncta. The overlay shows SV circle profiles of the both VGLUT1 and ZnT3 channels. Scale bar, 200 nm. **(E)** Representative confocal images of dendritic segments of hippocampal culture neurons labeled against VGLUT1, ZnT3 and Piccolo, a presynaptic active zone marker. Merge shows colocalization of the three proteins. Scale bar, 1 μ m. **(F)** Bar graph quantifying degree of colocalization between VGLUT1 and ZnT3 SVs in the WT mice. **(G)** Box plot showing significant spatial correlation between VGLUT1 and ZnT3 signals in comparison to their colocalization against Piccolo (**P<0.01 n = 3 experiments, unpaired t test). No significant difference observed for VGLUT1 and ZnT3 colocalization with respect to Piccolo (p=0.72, ns, unpaired t-test). Data in C and F are mean \pm SEM.

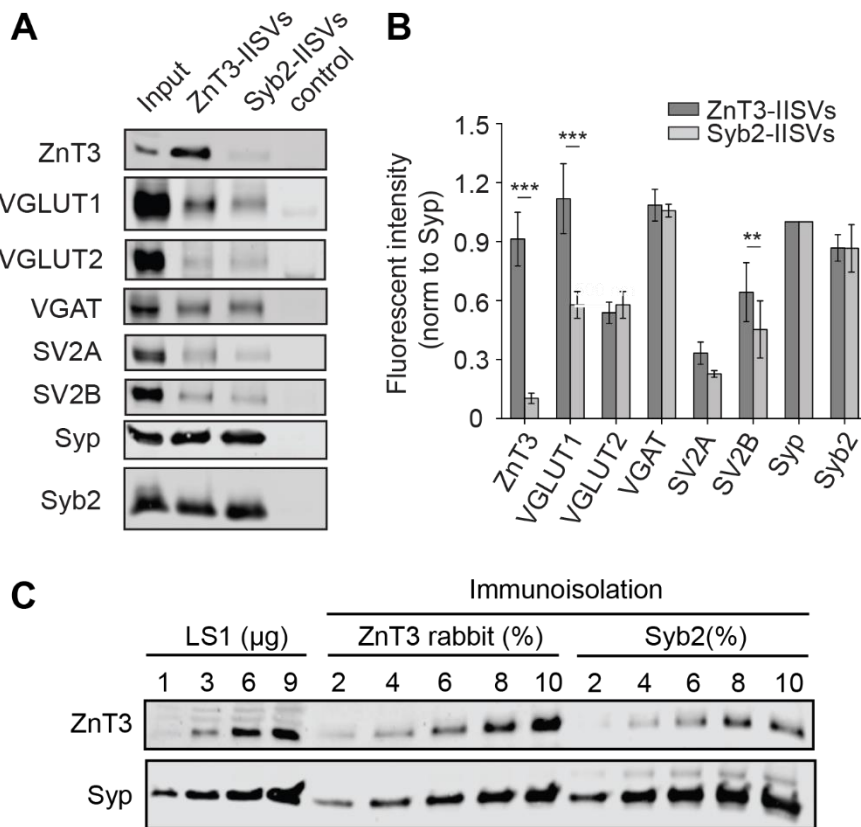


Figure S7. Immunisolated ZnT3 SVs show enrichment for VGLUT1 and SV2B

(A) Immunoblot showing differential enrichment of selected proteins in immunisolated SVs (IISVs) using specific antibodies against ZnT3 and Syb2 (substitute for all SVs). Note that only VGLUT1 and SV2B are enriched in ZnT3 immunisolated vesicles. (B) Summary bar graph showing significant enrichment of VGLUT1 and SV2B in ZnT3 immunisolated vesicles ($***P < 0.001$, $**P < 0.05$, $n = 3$ experiments, unpaired t-test) (C) Western blot analysis showing determination of loading volume for enrichment assay shown in B and C using Syp as reference. The experiment was performed on LS1, ZnT3 and Syb2 immunisolated samples for different loading volumes and detected against ZnT3 and Syp. The loading volume corresponding to equivalent Syp bands between ZnT3 and Syb2 samples were taken for western blot enrichment assay. Data are mean \pm SEM.